

See discussions, stats, and author profiles for this publication at: <https://www.researchgate.net/publication/231732358>

# Regioselective Bis-Selenation of Allenes Catalyzed by Palladium Complexes: A Theoretical Study

ARTICLE *in* ORGANOMETALLICS · MARCH 2009

Impact Factor: 4.13 · DOI: 10.1021/om801074s

---

CITATIONS

4

---

READS

16

## 4 AUTHORS, INCLUDING:



M. Wang

Chinese Academy of Sciences

13 PUBLICATIONS 172 CITATIONS

SEE PROFILE



Lin Cheng

Inner Mongolia University of Technology

18 PUBLICATIONS 111 CITATIONS

SEE PROFILE



Zhijian Wu

Chinese Academy of Sciences

236 PUBLICATIONS 2,519 CITATIONS

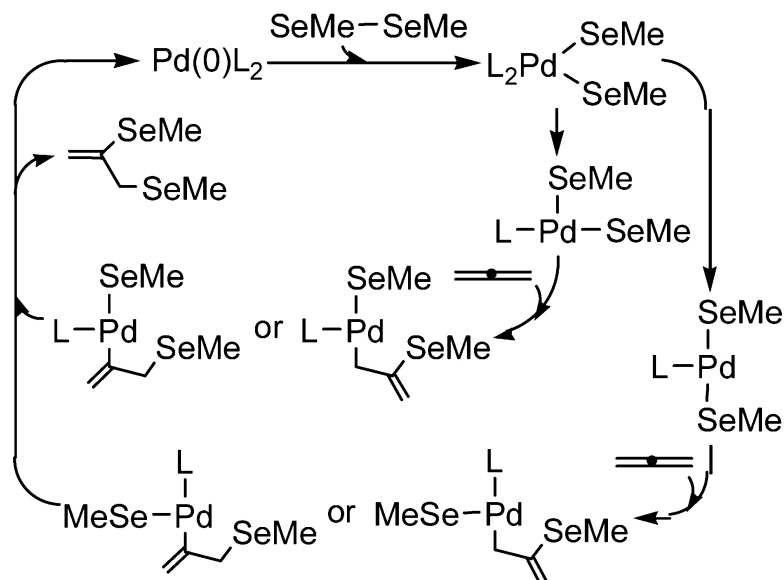
SEE PROFILE

## Regioselective Bis-Selenation of Allenes Catalyzed by Palladium Complexes: A Theoretical Study

Meiyan Wang, Lin Cheng, Bo Hong, and Zhijian Wu

*Organometallics*, **2009**, 28 (5), 1506-1513 • DOI: 10.1021/om801074s • Publication Date (Web): 29 January 2009

Downloaded from <http://pubs.acs.org> on March 3, 2009



### More About This Article

Additional resources and features associated with this article are available within the HTML version:

- Supporting Information
- Access to high resolution figures
- Links to articles and content related to this article
- Copyright permission to reproduce figures and/or text from this article

[View the Full Text HTML](#)



**ACS Publications**  
High quality. High impact.

*Organometallics* is published by the American Chemical Society, 1155 Sixteenth Street N.W., Washington, DC 20036

# Regioselective Bis-Selenation of Allenes Catalyzed by Palladium Complexes: A Theoretical Study

Meiyan Wang,<sup>†,‡</sup> Lin Cheng,<sup>†,‡</sup> Bo Hong,<sup>†,§</sup> and Zhijian Wu<sup>\*,†</sup>

State Key Laboratory of Rare Earth Resource Utilization, Changchun Institute of Applied Chemistry, Chinese Academy of Sciences, Changchun 130022, People's Republic of China, College of Resource and Environmental Science, Jilin Agricultural University, Changchun 130118, People's Republic of China, and Graduate School, Chinese Academy of Sciences, Beijing 100049, People's Republic of China

Received November 11, 2008

The reaction mechanism of Pd(0)-catalyzed allene bis-selenation reactions is investigated by using density functional methods. The overall reaction mechanism has been examined. It is found that with the bulkier PMe<sub>3</sub> ligand, the rate-determining step is the reductive elimination process, while allene insertion and reductive elimination processes are competitive for the rate-determining step with the PH<sub>3</sub> ligand, indicating the importance of the ligand effect. For both cis and trans palladium complexes, allene insertion into the Pd–Se bond of the trans palladium complex using the internal carbon atom attached to the selenyl group is preferred among the four pathways of allene insertion processes. The formation of  $\sigma$ -allyl and  $\pi$ -allyl palladium complexes is favored over that of the  $\sigma$ -vinyl palladium species. By using methylallene, the regioselectivity of monosubstituted allene insertion into the Pd–Se bond is analyzed. In addition, the influence of carbon monoxide on allene bis-selenation is studied by comparing the relevant transition states. It is found that carbon monoxide prefers to activate the Pd–C bond of the  $\sigma$ -vinyl palladium complex generated from allene insertion into the Pd–Se bond.

## I. Introduction

In recent years, considerable attention has been focused on the transition-metal-catalyzed addition of group 16 heteroatom compounds to carbon–carbon unsaturated bonds due to the increasing demand for sulfur- and selenium-containing compounds in organic chemistry and materials science.<sup>1–10</sup> In the past few decades, group 16 heteroatom compounds were not largely developed, probably because these compounds had long been considered as catalyst poisons due to their strong interaction with catalysts.<sup>11</sup> However, with the finding that, when catalyzed by palladium(0), disulfide and diselenide can add to carbon–carbon triple bonds to give the corresponding functional alkenes with high stereoselectivity,<sup>12,13</sup> more and more attention has been focused on the transition-metal-catalyzed addition of group 16 heteroatom compounds to unsaturated organic mol-

ecules. For sulfur-containing molecules, S–S and S–H bond additions to alkynes or allenes have been developed to obtain the vinyl and allyl sulfur compounds.<sup>12–25</sup> For selenium-containing molecules, catalytic additions to alkynes have been the most studied,<sup>12,13,26–31</sup> while there have been few additions to allenes.<sup>22–24,32,33</sup> The bis-selenation of allenes can be

\* To whom correspondence should be addressed. Fax: +86-431-85698041. E-mail: zjwu@ciac.jl.cn.

<sup>†</sup> Changchun Institute of Applied Chemistry, Chinese Academy of Sciences.

<sup>‡</sup> Graduate School, Chinese Academy of Sciences.

<sup>§</sup> Jilin Agricultural University.

- (1) Beletskaya, I. P.; Ananikov, V. P. *Eur. J. Org. Chem.* **2007**, 3431.
- (2) Ogawa, A.; Sonoda, N. *J. Synth. Org. Chem., Jpn.* **1993**, 51, 815.
- (3) Ogawa, A. *J. Organomet. Chem.* **2000**, 611, 463.
- (4) Alonso, F.; Beletskaya, I. P.; Yus, M. *Chem. Rev.* **2004**, 104, 3079.
- (5) Kondo, T.; Mitsudo, T. *Chem. Rev.* **2000**, 100, 3205.
- (6) Han, L.-B.; Tanaka, M. *Chem. Commun.* **1999**, 395.
- (7) Beletskaya, I.; Moberg, C. *Chem. Rev.* **1999**, 99, 3435.
- (8) Beletskaya, I.; Moberg, C. *Chem. Rev.* **2006**, 106, 2320.
- (9) Kuniyasu, H.; Kambe, N. *Chem. Lett.* **2006**, 35, 1320.
- (10) Kuniyasu, H. *Catalytic Heterofunctionalization*; Togni, A., Grützmacher, H., Eds.; Wiley-VCH: Zürich, Switzerland, 2001; p 217.
- (11) Hegedus, L. L.; McCabe, R. W. *Catalyst Poisoning*; Marcel Dekker: New York, 1984.
- (12) Kuniyasu, H.; Ogawa, A.; Miyazaki, S.-I.; Ryu, I.; Kambe, N.; Sonoda, N. *J. Am. Chem. Soc.* **1991**, 113, 9796.
- (13) Ogawa, A.; Kuniyasu, H.; Sonoda, N.; Hirao, T. *J. Org. Chem.* **1997**, 62, 8361.

- (14) Ogawa, A.; Kawakami, J.; Mihara, M.; Ikeda, T.; Sonoda, N.; Hirao, T. *J. Am. Chem. Soc.* **1997**, 119, 12380.
- (15) Arisawa, M.; Yamaguchi, M. *Org. Lett.* **2001**, 3, 763.
- (16) Gareau, Y.; Orellana, A. *Synlett* **1997**, 803.
- (17) Xiao, W.-J.; Alper, H. *J. Org. Chem.* **2005**, 70, 1802.
- (18) Kawakami, J.; Mihara, M.; Kamiya, I.; Takeba, M.; Ogawa, A.; Sonoda, N. *Tetrahedron* **2003**, 59, 3521.
- (19) Kawakami, J.; Takeba, M.; Kamiya, I.; Sonoda, N.; Ogawa, A. *Tetrahedron* **2003**, 59, 6559.
- (20) Ogawa, A.; Takeba, M.; Kawakami, J.; Ryu, I.; Kambe, N.; Sonoda, N. *J. Am. Chem. Soc.* **1995**, 117, 7564.
- (21) Kajitani, M.; Kamiya, I.; Nomoto, A.; Kihara, N.; Ogawa, A. *Tetrahedron* **2006**, 62, 6355.
- (22) Ogawa, A.; Yokoyama, K.; Yokoyama, H.; Sekiguchi, M.; Kambe, N.; Sonoda, N. *Tetrahedron Lett.* **1990**, 31, 5931.
- (23) Arisawa, M.; Suwa, A.; Fujimoto, K.; Yamaguchi, M. *Adv. Synth. Catal.* **2003**, 345, 560.
- (24) Kodama, S.; Nishinaka, E.; Nomoto, A.; Sonoda, M.; Ogawa, A. *Tetrahedron Lett.* **2007**, 48, 6312.
- (25) Ogawa, A.; Kawakami, J.; Sonoda, N.; Hirao, T. *J. Org. Chem.* **1996**, 61, 4161.
- (26) Ananikov, V. P.; Orlov, N. V.; Kabeshov, M. A.; Beletskaya, I. P.; Starikova, Z. A. *Organometallics* **2008**, 27, 4056.
- (27) Kamiya, I.; Nishinaka, E.; Ogawa, A. *J. Org. Chem.* **2005**, 70, 696.
- (28) Ananikov, V. P.; Malyshev, D. A.; Beletskaya, I. P.; Aleksandrov, G. G.; Eremenko, I. L. *J. Organomet. Chem.* **2003**, 679, 162.
- (29) Ananikov, V. P.; Kabeshov, M. A.; Beletskaya, I. P.; Aleksandrov, G. G.; Eremenko, I. L. *J. Organomet. Chem.* **2003**, 687, 451.
- (30) Kuniyasu, H.; Ogawa, A.; Higaki, K.; Sonoda, N. *Organometallics* **1992**, 11, 3937.
- (31) Ananikov, V. P.; Beletskaya, I. P.; Aleksandrov, G. G.; Eremenko, I. L. *Organometallics* **2003**, 22, 1414.
- (32) Ogawa, A.; Kudo, A.; Hirao, T. *Tetrahedron Lett.* **1998**, 39, 5213.
- (33) Kamiya, I.; Nishinaka, E.; Ogawa, A. *Tetrahedron Lett.* **2005**, 46, 3649.

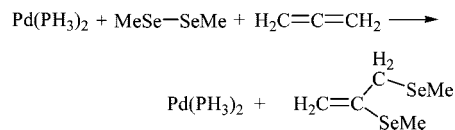
conducted under photoirradiated radical conditions<sup>22</sup> or by use of transition-metal catalysts.<sup>33</sup>

Palladium-catalyzed bis-selenation of allenes<sup>33</sup> was first reported by Ogawa and co-workers in 2005. Highly regioselective addition products are obtained with two selenyl groups attached to the terminal carbon–carbon double bond of the allenes. This regioselectivity is special, because the addition of Si–Si, Sn–Sn, Si–Sn, B–B, and B–Si bonds to allenes generates organic compounds with two functional groups added to the internal carbon–carbon double bond of allenes.<sup>8</sup> To study the reaction mechanism, bis-selenation of allenes was conducted in the presence of carbon monoxide.<sup>33</sup> The carbonyl group was thus introduced into the product compounds. Although the carbonylated product with carbonyl between the selenyl group and the internal carbon atom was obtained, the product with carbonyl between the selenyl group and the terminal carbon atom was not. In accord with the carbonylated products, the reaction was suggested to proceed via oxidative addition, allene insertion into the Pd–Se bond to provide the  $\sigma$ -vinyl palladium intermediate, and finally reductive elimination.<sup>33</sup> However, in comparison with the mechanisms of transition-metal-catalyzed diboration, silaboration, and silastannation of allenes in which the  $\pi$ -allyl intermediates are formed selectively,<sup>8</sup> the suggested allene bis-selenation mechanism in the experiment<sup>33</sup> is found to be different.

The theoretical aspects of the palladium-catalyzed silaboration of methylallene have been studied.<sup>34</sup> It was found that methylallene prefers to insert into the Pd–B bond, generating the  $\pi$ -allyl palladium intermediate. For the oxidative addition of group 16 heteroatom compounds to transition-metal complexes, S–S and Se–Se bonds to nickel and palladium complexes<sup>35</sup> and S–S, Se–Se, and Te–Te bonds to palladium and platinum complexes have been investigated.<sup>36</sup> The activation of Se–Se bonds by palladium complexes, generating Se=PPh<sub>3</sub> and PhSePh complexes, has been studied.<sup>37</sup> Recently, nickel-catalyzed S–S and Se–Se bond addition to alkynes has been studied both experimentally and theoretically.<sup>26</sup> Through calculations, it was found that the Ni–C bond is preferred to the Ni–S bond for alkyne insertion. In addition, palladium-catalyzed addition of the Se–C(O) bond to allenes has been conducted to give functionalized allyl selenides with carbonyl at the internal carbon and a selenyl group at the terminal carbon.<sup>38</sup> It was found that Pd–C(O)Me is preferred over Pd–Se for allene insertion.

Although the reaction mechanism of the bis-selenation of allenes was proposed by experiment,<sup>33</sup> the detailed reaction process remains unclear. To understand the reaction mechanism, it is interesting to know which carbon atom, the terminal carbon atom or the internal carbon of allene, is preferred to attach to selenyl during allene insertion into the Pd–Se bond. Since the bis-selenation of allene was conducted in the presence of carbon monoxide, it would be also interesting to know how carbon monoxide influences the bis-selenation reaction.

To understand the detailed mechanism of the Pd(0)-catalyzed allene bis-selenation process, we have carried out theoretical calculations for the model reaction



In the model reaction, the PPh<sub>3</sub> ligand in the catalyst Pd(PPh<sub>3</sub>)<sub>2</sub> was simplified to PH<sub>3</sub>, while MeSe–SeMe and allene CH<sub>2</sub>=C=CH<sub>2</sub> were models for diselenides and substituted allenes in experiment.<sup>33</sup> The simplification of PPh<sub>3</sub> to PH<sub>3</sub> was adopted by many previous studies and was shown to be reasonable for the study of the reaction mechanism.<sup>26,34–38</sup> In addition, in previous studies MeSe–SeMe was also a reasonable model for diphenyl diselenides.<sup>26,35–38</sup>

## II. Computational Methods

All calculations were performed using the Gaussian 03 suite of programs.<sup>39</sup> Geometries of the stationary points and transition states on the energy profiles were optimized by use of the hybrid density functional method (DFT) B3LYP<sup>40–42</sup> and pure density functional method BP86.<sup>40,43</sup> For the basis set, double- $\zeta$  LANL2DZ was used for Pd and Se atoms, in which the effective core potentials (ECP) were used and mass–velocity and Darwin relativistic effects were incorporated.<sup>44</sup> For the remaining elements (i.e., C, H, O, and P atoms), the standard 6-311G(d) basis set was adopted. We denote the combination of the two basis sets (LANL2DZ for Pd and Se, 6-311G(d) for the remaining atoms) as BSI. The optimization was carried out without imposing any symmetry constraints. Harmonic vibrational frequencies and thermal corrections to free energies were obtained at the same level of theory. Relative free energies were obtained by performing single-point calculations at the B3LYP (and BP86) level with LANL2DZ plus f-polarization<sup>45</sup> with an exponent of 1.472 for Pd, d-polarization<sup>46</sup> with an exponent of 0.338 for Se, and the 6-311+G(d,p) basis set for the remaining atoms (the combination of the two basis sets is named as BSII) using the above optimized geometries and by including thermal corrections to free energies at B3LYP/BSI (and BP86/BSI), which includes entropy contributions by taking into account the vibrational, rotational, and translational motions of the species at 298.15 K. The stationary points and transition states on the energy profiles were confirmed by normal-mode analysis. The intrinsic reaction coordinate (IRC) approach was used to confirm that the transition state indeed connects two relevant minima.<sup>47,48</sup>

(40) Becke, A. D. *Phys. Rev. A* **1988**, *38*, 3098.

(41) Lee, C.; Yang, W.; Parr, R. G. *Phys. Rev. B* **1988**, *37*, 785.

(42) Becke, A. D. *J. Chem. Phys.* **1993**, *98*, 5648.

(43) Perdew, J. P. *Phys. Rev. B* **1986**, *33*, 8822.

(44) Hay, P. J.; Wadt, W. R. *J. Chem. Phys.* **1985**, *82*, 299.

(45) Ehlers, A. W.; Böhme, M.; Dapprich, S.; Gobbi, A.; Höllwarth, A.; Jonas, V.; Köhler, K. F.; Stegmann, R.; Veldkamp, A.; Frenking, G. *Chem. Phys. Lett.* **1993**, *208*, 111.

(46) *Gaussian Basis Sets for Molecular Calculations*; Huzinaga, S., Ed.; Elsevier Science: Amsterdam, 1984.

(47) Fukui, K. *J. Phys. Chem.* **1970**, *74*, 4161.

(34) Abe, Y.; Kuramoto, K.; Ehara, M.; Nakatsuji, H.; Sugimoto, M.; Murakami, M.; Ito, Y. *Organometallics* **2008**, *27*, 1736.

(35) Ananikov, V. P.; Gayduk, K. A.; Beletskaya, I. P.; Khrustalev, V. N.; Antipin, M. Y. *Chem. Eur. J.* **2008**, *14*, 2420.

(36) Gonzales, J. M.; Musaev, D. G.; Morokuma, K. *Organometallics* **2005**, *24*, 4908.

(37) Ananikov, V. P.; Orlov, N. V.; Beletskaya, I. P. *Russ. Chem. Bull. Int. Ed.* **2005**, *54*, 576.

(38) Toyofuku, M.; Murase, E.; Fujiwara, S.; Shin-ike, T.; Kuniyasu, H.; Kambe, N. *Org. Lett.* **2008**, *10*, 3957.

(39) Frisch, M. J.; Trucks, G. W.; Schlegel, H. B.; Scuseria, G. E.; Robb, M. A.; Cheeseman, J. R.; Montgomery, J. A., Jr.; Vreven, T.; Kudin, K. N.; Burant, J. C.; Millam, J. M.; Iyengar, S. S.; Tomasi, J.; Barone, V.; Mennucci, B.; Cossi, M.; Scalmani, G.; Rega, N.; Petersson, G. A.; Nakatsuji, H.; Hada, M.; Ehara, M.; Toyota, K.; Fukuda, R.; Hasegawa, J.; Ishida, M.; Nakajima, T.; Honda, Y.; Kitao, O.; Nakai, H.; Klene, M.; Li, X.; Knox, J. E.; Hratchian, H. P.; Cross, J. B.; Adamo, C.; Jaramillo, J.; Gomperts, R.; Stratmann, R. E.; Yazyev, O.; Austin, A. J.; Cammi, R.; Pomelli, C.; Ochterski, J. W.; Ayala, P. Y.; Morokuma, K.; Voth, G. A.; Salvador, P.; Dannenberg, J. J.; Zakrzewski, V. G.; Dapprich, S.; Daniels, A. D.; Strain, M. C.; Farkas, O.; Malick, D. K.; Rabuck, A. D.; Raghavachari, K.; Foresman, J. B.; Ortiz, J. V.; Cui, Q.; Baboul, A. G.; Clifford, J.; Cioslowski, J.; Stefanov, B. B.; Liu, G.; Liashenko, A.; Piskorz, P.; Komaromi, I.; Martin, R. L.; Fox, D. J.; Keith, T.; Al-Laham, M. A.; Peng, C. Y.; Nanayakkara, A.; Challacombe, M.; Gill, P. M. W.; Johnson, B.; Chen, W.; Wong, M. W.; Gonzalez, C.; Pople, J. A. *Gaussian 03*; Gaussian, Inc., Pittsburgh, PA, 2003.

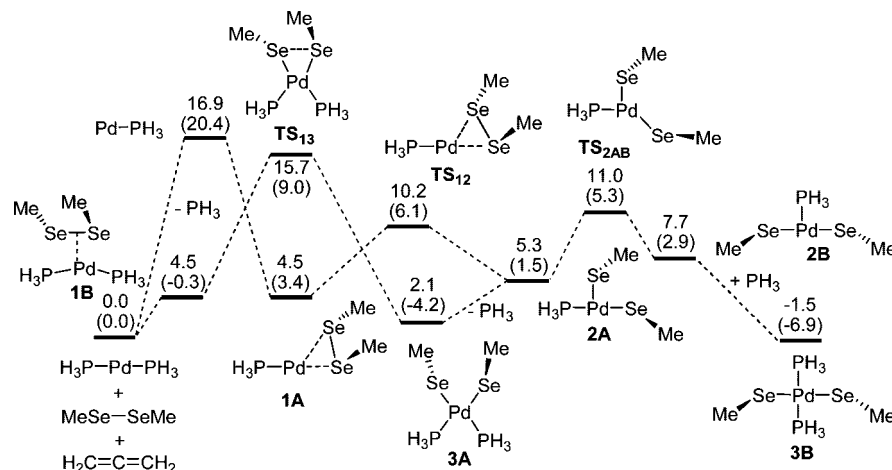
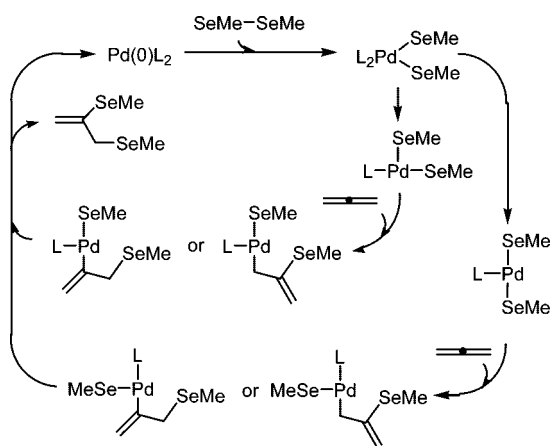


**Figure 1.** Calculated energy profiles for the oxidative addition of MeSe–SeMe to Pd(PH<sub>3</sub>) (Pd(PH<sub>3</sub>) → **1A** → **2A**) and Pd(PH<sub>3</sub>)<sub>2</sub> (Pd(PH<sub>3</sub>)<sub>2</sub> → **1B** → **3A** → **2A**) and isomerization between cis complex **3A** and trans complex **3B**. The energy values (in kcal/mol) are the relative free energies from B3LYP, while those in parentheses are from BP86.

**Scheme 1. Proposed Mechanism for the Pd(PH<sub>3</sub>)<sub>2</sub>-Catalyzed Bis-Selenation of Allene**



Previous benchmark calculations<sup>49–52</sup> have demonstrated that B3LYP is reasonable in estimating the transition barriers (close to ab initio results) in the study of oxidative addition and reductive elimination processes as they occur in the present study, while BP86 tends to underestimate the transition barriers.<sup>49–52</sup> Therefore, in this paper, our discussion will focus on the B3LYP results, while BP86 values are used for comparison. The energies are all given in kcal/mol.

### III. Results and Discussion

The proposed mechanism of Pd(0)-catalyzed allene bis-selenation reaction was presented in Scheme 1. In this mechanism, Se–Se bond oxidative addition to the Pd(0) complex to form the Pd–Se bond occurs first. The Se–Se bond oxidative addition product with two selenyl groups in cis positions can undergo isomerization to the trans isomer. Thus, both the cis and trans palladium species have been examined for allene coordination

and insertion. For the cis species, allene insertion into the Pd–Se bond using either the terminal or internal carbon atom attached to the selenyl group takes two pathways, generating the  $\sigma$ -vinyl and  $\sigma$ -allyl palladium complexes. For the trans species, there are also two pathways for allene insertion into the Pd–Se bond. After the allene insertion, the other selenyl group migrates to allene through a reductive elimination process to form the final addition product.

**A. Oxidative Addition and Isomerization.** From previous theoretical studies of MeSe–SeMe oxidative addition to nickel<sup>35</sup> and palladium<sup>35,37</sup> complexes, the Se–Se bond activation is more favorable than C–Se bond activation; thus, only the activation of the Se–Se bond is considered in the oxidative addition step. Both mono-phosphine (Pd(PH<sub>3</sub>)) and bis-phosphine (Pd(PH<sub>3</sub>)<sub>2</sub>) pathways have been investigated for Se–Se bond activation (Figure 1). In the mono-phosphine pathway, the dissociation of PH<sub>3</sub> from Pd(PH<sub>3</sub>)<sub>2</sub> costs an energy of 16.9 kcal/mol, forming Pd(PH<sub>3</sub>). After that, MeSe–SeMe coordination to Pd(PH<sub>3</sub>) gives the complex **1A**, from which complex **2A** is generated via transition state **TS**<sub>12</sub> with an energy barrier of 5.7 kcal/mol. In the bis-phosphine pathway, the MeSe–SeMe molecule initially coordinates to the Pd atom of Pd(PH<sub>3</sub>)<sub>2</sub>, forming the structure **1B**. From **1B**, the Se–Se bond in MeSe–SeMe is activated through transition state **TS**<sub>13</sub>, forming the bis-selenyl palladium(II) oxidative addition product **3A** with two selenyl groups in cis positions. The energy barrier of **TS**<sub>13</sub> relative to the separated system or the initial reactants is calculated to be 15.7 kcal/mol. The dissociation of PH<sub>3</sub> from complex **3A** forms complex **2A**. On comparison of the mono-phosphine pathway Pd(PH<sub>3</sub>)<sub>2</sub> → Pd(PH<sub>3</sub>) → **1A** → **2A**, with an energy barrier of 16.9 kcal/mol, to the bis-phosphine pathway, Pd(PH<sub>3</sub>)<sub>2</sub> → **1B** → **3A** → **2A**, with an energy barrier of 15.7 kcal/mol, the bis-phosphine pathway is only slightly preferred over the mono-phosphine pathway. On the other hand, at the pure DFT method BP86 level, **TS**<sub>13</sub> is much lower (by 11.4 kcal/mol) than Pd(PH<sub>3</sub>). Thus, the pathway Pd(PH<sub>3</sub>)<sub>2</sub> → **1B** → **3A** → **2A** is favored over Pd(PH<sub>3</sub>)<sub>2</sub> → Pd(PH<sub>3</sub>) → **1A** → **2A**.

In the three-coordinate complex **2A**, the two selenyl groups are cis to each other. The isomerization of **2A** takes place via transition state **TS**<sub>2AB</sub> with an energy barrier of 8.9 kcal/mol relative to **3A**, forming the isomer **2B** with two selenyl groups trans to each other (Figure 1). Reoordination of one phosphine to complex **2B** generates the trans complex **3B**. In complexes **2A** and **3A**, the two selenyl groups are cis to each other, while

(48) Fukui, K. *Acc. Chem. Res.* **1981**, *14*, 363.

(49) de Jong, G. T.; Geerke, D. P.; Diefenbach, A.; Bickelhaupt, F. M. *Chem. Phys.* **2005**, *313*, 261.

(50) de Jong, G. T.; Geerke, D. P.; Diefenbach, A.; Solà, M.; Bickelhaupt, F. M. *J. Comput. Chem.* **2005**, *26*, 1006.

(51) de Jong, G. T.; Bickelhaupt, F. M. *J. Phys. Chem. A* **2005**, *109*, 9685.

(52) de Jong, G. T.; Bickelhaupt, F. M. *J. Chem. Theory Comput.* **2006**, *2*, 322.



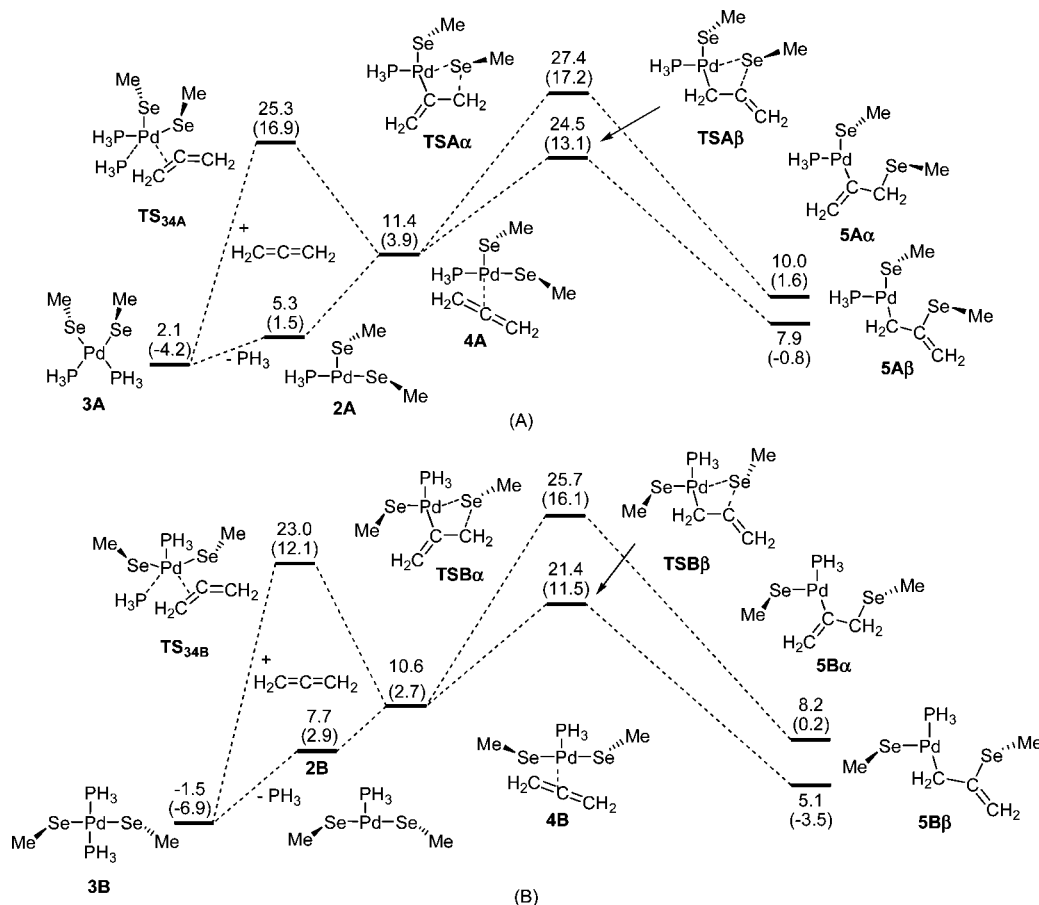


**Figure 2.** Calculated energy profiles for allene coordination and insertion into the Pd–Se bond of the cis complex (A) and trans complex (B). The energy values (in kcal/mol) are the relative free energies from B3LYP, while those in parentheses are from BP86. All values are relative to the initial reactants  $\text{Pd}(\text{PH}_3)_2 + \text{MeSe-SeMe} + \text{CH}_2=\text{C}=\text{CH}_2$ .

they are trans in complexes **2B** and **3B**. The trans complex **3B** is 3.6 kcal/mol more stable than cis complex **3A** (this is also true when the bulkier ligand  $\text{PMe}_3$  is considered: i.e., **3B** is more stable than **3A** by 6.4 kcal/mol). Complex **2B** is slightly (2.4 kcal/mol at B3LYP, 1.4 kcal/mol at BP86) higher than **2A**, and the energy difference between  $\text{TS}_{2AB}$  and **2A** is only 5.7 kcal/mol at B3LYP or 3.8 kcal/mol at BP86. Thus, both the cis and trans complexes should be examined for allene coordination and insertion.

**B. Allene Coordination and Insertion.** The next step is the coordination and insertion of allene at the bis(selenyl)palladium(II) complex, producing the  $\sigma$ -vinyl or  $\sigma$ -allyl palladium complex (Figure 2). For allene coordination, there are two kinds of pathways. The first is the direct coordination of allene to complex **2A** or **2B**. The other is the phosphine dissociation from **3A** (or **3B**) and allene coordination to **3A** (or **3B**) taking place simultaneously.

The coordination of allene to cis complex **2A** generates complex **4A** (Figure 2A). The phosphine dissociation and allene coordination to **3A** occur at the five-coordinate transition state  $\text{TS}_{34A}$  with an energy barrier of 23.2 kcal/mol to form **4A**. It is clear that the pathway  $3A \rightarrow 2A \rightarrow 4A$  is preferred over  $3A \rightarrow \text{TS}_{34A} \rightarrow 4A$ . From complex **4A**, the insertion of allene proceeds through two routes, depending on the different orientations of the carbon–carbon double bond of allene relative to the Pd–Se bond. Allene insertion into the Pd–Se bond using the terminal carbon atom attached to selenyl takes place with a barrier of 25.3 kcal/mol at  $\text{TS}_{A\alpha}$  relative to **3A**, giving the  $\sigma$ -vinyl complex **5A $\alpha$** , while allene insertion into the Pd–Se bond using the internal carbon atom connected to selenyl takes place with

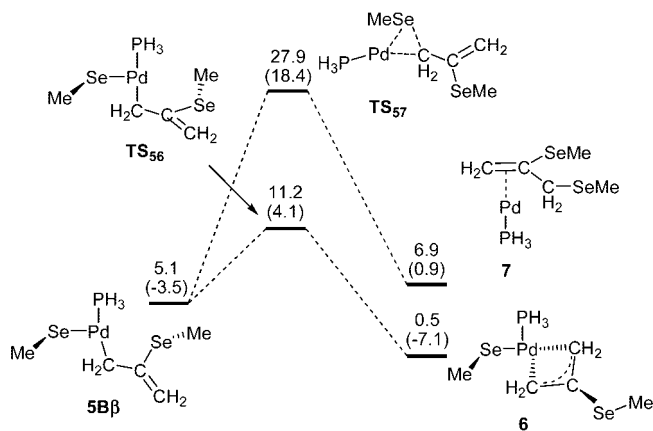


**Figure 3.** Calculated energy profiles for isomerization and reductive elimination from complex **5B $\beta$** . The energy values (in kcal/mol) are the relative free energies from B3LYP, while those in parentheses are from BP86. All values are relative to the initial reactants.

a barrier of 22.4 kcal/mol at  $\text{TS}_{A\beta}$  relative to **3A**, giving the  $\sigma$ -allyl complex **5A $\beta$**  (Figure 2A). The transition state  $\text{TS}_{A\alpha}$  is 2.9 kcal/mol higher than  $\text{TS}_{A\beta}$ . Therefore, the pathway  $4A \rightarrow \text{TS}_{A\beta} \rightarrow 5A\beta$  is favored over  $4A \rightarrow \text{TS}_{A\alpha} \rightarrow 5A\alpha$ .

The pathways of allene coordination to the trans complexes **2B** and **3B** and insertion into the Pd–Se bond (Figure 2B) are similar to those for cis complexes **2A** and **3A** (Figure 2A). It is clear that the pathway  $3B \rightarrow 2B \rightarrow 4B$  is preferred over  $3B \rightarrow \text{TS}_{34B} \rightarrow 4B$  and  $4B \rightarrow \text{TS}_{B\beta} \rightarrow 5B\beta$  is favored over  $4B \rightarrow$

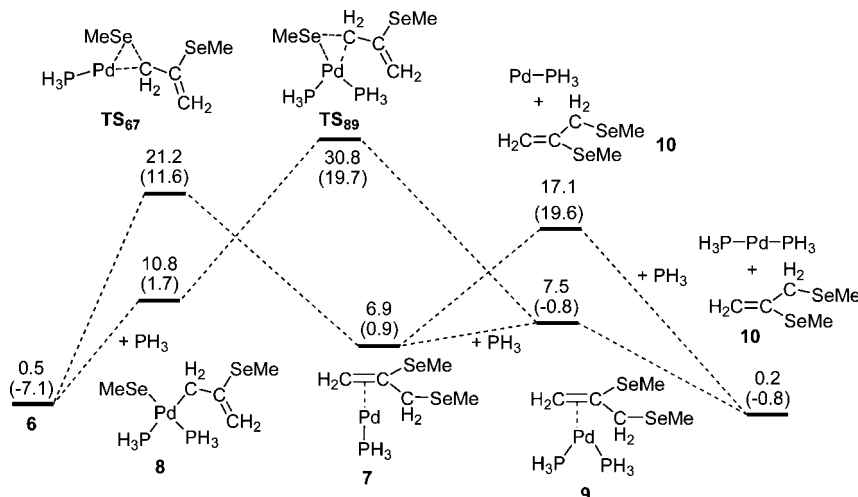


**Figure 4.** Calculated energy profiles for reductive elimination from complex **6** through the mono-phosphine (**6**  $\rightarrow$  **7**  $\rightarrow$  **9**  $\rightarrow$  **10**) and bis-phosphine (**6**  $\rightarrow$  **8**  $\rightarrow$  **9**  $\rightarrow$  **10**) pathways. The energy values (in kcal/mol) are the relative free energies from B3LYP, while those in parentheses are from BP86. All values are relative to the initial reactants.

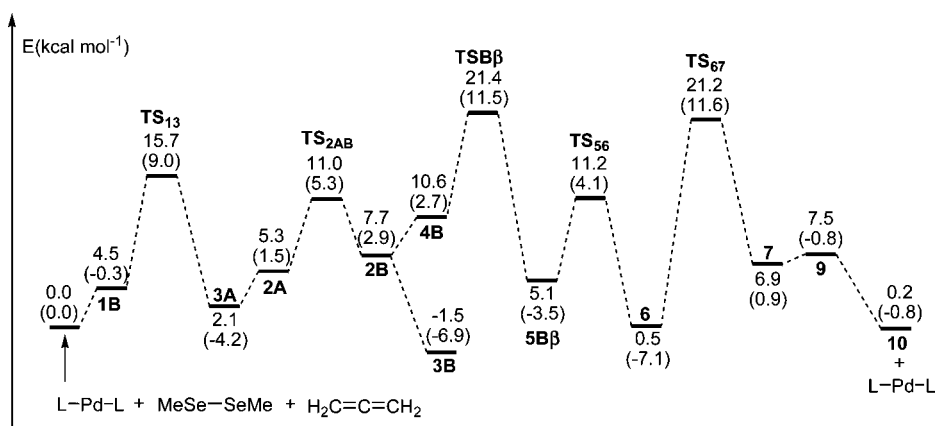


**Figure 5.** Calculated energy profiles for the overall reaction of allene bis-selenation catalyzed by  $\text{Pd}(\text{PH}_3)_2$ . The energy values (in kcal/mol) are the relative free energies from B3LYP, while those in parentheses are from BP86.

**TSB $\alpha$   $\rightarrow$  5B $\alpha$ .** Among the four pathways of allene insertion into the Pd–Se bond, the energy of transition state **TSB $\beta$**  is lowest, and complex **5B $\beta$**  is most stable among the four insertion products. Therefore, the pathway **4B**  $\rightarrow$  **TSB $\beta$**   $\rightarrow$  **5B $\beta$**  is favored both kinetically and thermodynamically. In addition, from BP86 results, the pathway **4B**  $\rightarrow$  **TSB $\beta$**   $\rightarrow$  **5B $\beta$**  is also preferred both kinetically and thermodynamically. In other words, the trans complex is favored over the cis complex for allene insertion into the Pd–Se bond and the internal carbon atom of allene is preferred over the terminal carbon atom to attach to the selenyl group during allene insertion. This is consistent with the theoretical results<sup>34</sup> of methylallene silaboration, in which the internal carbon atom is also preferred to attach to the boryl group in the methylallene insertion step. The preference of the trans complex for allene insertion has also been noted in alkyne insertion into the Pt–S bond,<sup>53</sup> in which *trans*-Pt(SAr)<sub>2</sub>(PPh<sub>3</sub>)<sub>2</sub> has a higher reactivity than *cis*-Pt(SAr)<sub>2</sub>(PPh<sub>3</sub>)<sub>2</sub> under both thermal and photoirradiated reaction conditions.<sup>53</sup>

**C. Isomerization from  $\sigma$ -Allyl to  $\pi$ -Allyl Complex.** The  $\sigma$ -allyl complex **5B $\beta$**  has an approximately planar structure with selenyl and allyl groups located in a *cis* orientation. A conversion from the  $\sigma$ -allyl complex to the  $\pi$ -allyl complex in the

silaboration of allenes was initially proposed by Sugimoto et al. from experiment<sup>54</sup> and demonstrated later by a theoretical study.<sup>34</sup> Thus, this  $\sigma$ -allyl to  $\pi$ -allyl isomerization is examined. The isomerization of  $\sigma$ -allyl complex **5B $\beta$**  takes place via transition state **TS<sub>56</sub>** with a barrier of 6.1 kcal/mol, generating the  $\pi$ -allyl complex **6** (Figure 3). Since selenyl and allyl groups are *cis* to each other in **5B $\beta$** , the reductive elimination from complex **5B $\beta$**  could take place directly. The reductive elimination from **5B $\beta$** , generating complex **7** via transition state **TS<sub>57</sub>**, has an energy barrier of 22.8 kcal/mol. On comparison of the two pathways from complex **5B $\beta$** , the isomerization from the  $\sigma$ -allyl to  $\pi$ -allyl complex is favored.

**D. Reductive Elimination.** In complex **6**, the selenyl and allyl groups are *cis* to each other (Figure 3), and reductive elimination can proceed through two pathways: i.e., mono-phosphine and bis-phosphine pathways (Figure 4). In the mono-phosphine pathway, reductive elimination takes place directly through the transition state **TS<sub>67</sub>** with a barrier of 20.7 kcal/mol to form complex **7**. In the bis-phosphine pathway, the recoordination of  $\text{PH}_3$  generates complex **8**, from which the reductive elimination takes place via transition state **TS<sub>89</sub>** with a barrier of 30.3 kcal/mol relative to **6**, forming complex **9**. The dissociation of  $\text{Pd}(\text{PH}_3)$  and  $\text{Pd}(\text{PH}_3)_2$  from the  $\pi$ -vinyl

(53) Kuniyasu, H.; Takekawa, K.; Yamashita, F.; Miyafuji, K.; Asano, S.; Takai, Y.; Ohtaka, A.; Tanaka, A.; Sugoh, K.; Kurosawa, H.; Kambe, N. *Organometallics* **2008**, *27*, 4788.

(54) Sugimoto, M.; Ohmori, Y.; Ito, Y. *J. Organomet. Chem.* **2000**, *611*, 403.

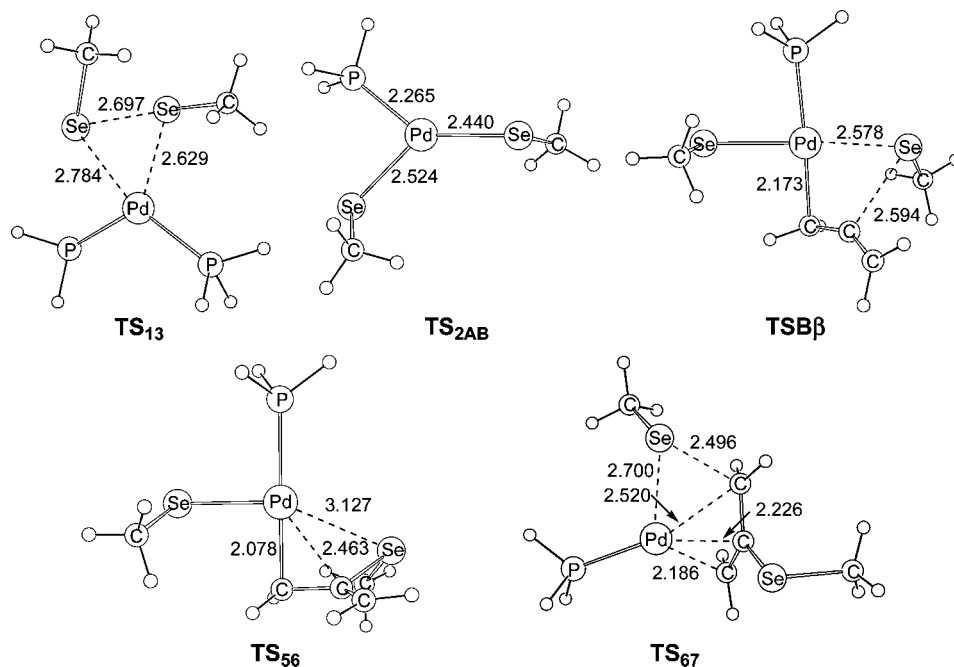
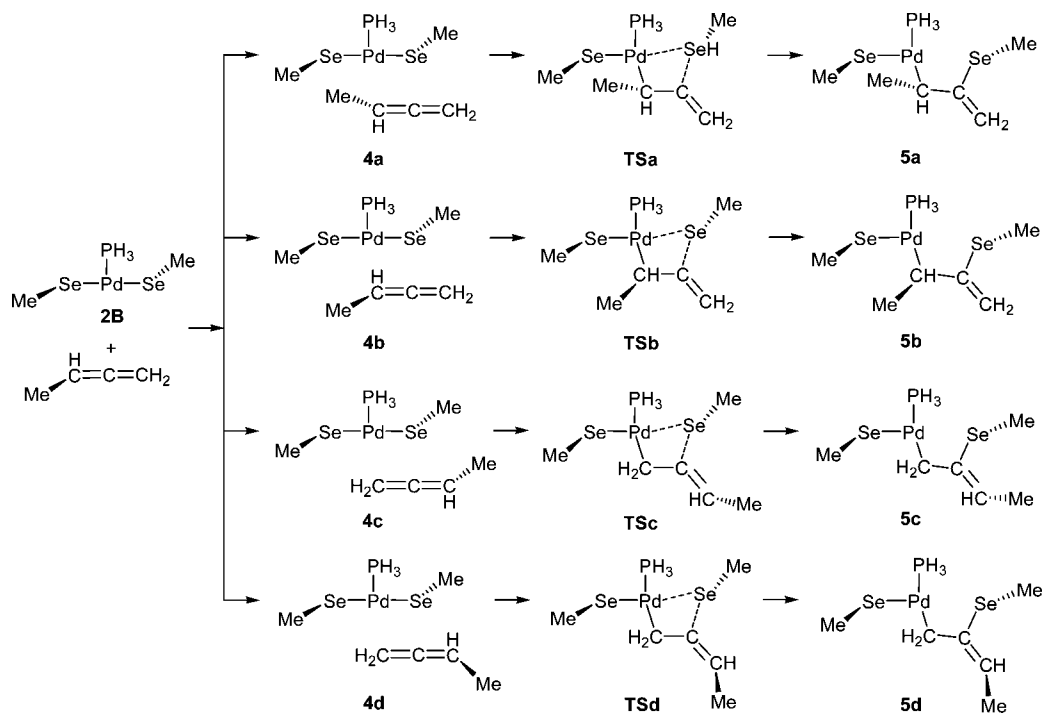


Figure 6. Selected geometries (Å) in the overall reaction profile of Figure 5 (five transition states).

**Scheme 2. Proposed Mechanism for Methylallene Insertion into the Pd–Se Bond of Complex 2B**



complexes **7** and **9** generates the final product (Z)-CH<sub>2</sub>=C(SeMe)CH<sub>2</sub>(SeMe) (**10**). In addition, recoordination of PH<sub>3</sub> to **7** generates **9**. Transition state TS<sub>89</sub> is 9.6 kcal/mol higher than TS<sub>67</sub> (Figure 4). Therefore, it is clear that the reductive elimination of **10** prefers to proceed through the monophosphine pathway **6** → **7** → **9** → **10**. At the BP86 level, the pathway **6** → **7** → **9** → **10** is also preferred for reductive elimination.

From previous studies, the ionic intermediate [Pd( $\eta^3$ -CH<sub>2</sub>CRCH<sub>2</sub>)(PPh<sub>3</sub>)<sub>2</sub>]<sup>+</sup>PhS<sup>−</sup> had been proposed for the C–S bond formation.<sup>55</sup> Although not examined, a similar ionic

intermediate for the C–Se bond formation, [Pd( $\eta^3$ -CH<sub>2</sub>-CRCH<sub>2</sub>)(PH<sub>3</sub>)<sub>2</sub>]<sup>+</sup>MeSe<sup>−</sup> (generated from **6**), might also be possible.

**E. Reaction Mechanism.** The overall reaction profile for addition of an Se–Se bond to the carbon–carbon double bond of allene catalyzed by Pd(PH<sub>3</sub>)<sub>2</sub> is presented in Figure 5. The geometries of selected key structures (five transition states) are given in Figure 6. From Figure 5, it is found that the insertion transition state TSB $\beta$  and reductive elimination transition state TS<sub>67</sub> are the two highest transition states on the reaction profile. TSB $\beta$  is only 0.2 kcal/mol higher than TS<sub>67</sub> at B3LYP, while it is 0.1 kcal/mol lower at BP86. This indicates that allene insertion and reductive elimination are comparable for the rate-

(55) Miyauchi, Y.; Watanabe, S.; Kuniyasu, H.; Kurosawa, H. *Organometallics* **1995**, *14*, 5450.



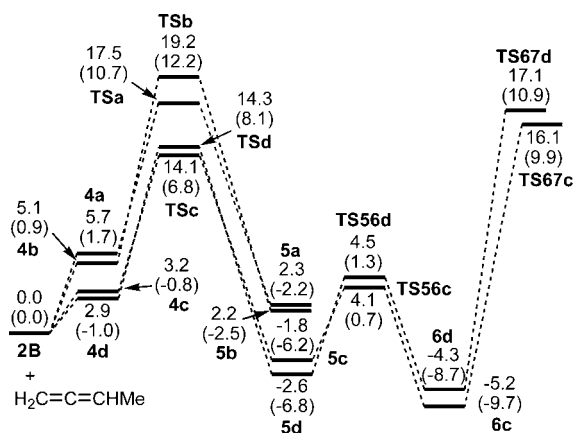


**Figure 7.** Calculated energy profiles for methylallene insertion into the Pd–Se bond of complex **2B**. The energy values (in kcal/mol) are the relative free energies from B3LYP, while those in parentheses are from BP86. All values are relative to the initial reactants **2B** +  $\text{H}_2\text{C}=\text{C}=\text{CHMe}$ .

determining step with the  $\text{PH}_3$  ligand. Thus, the bulkier phosphine ligand  $\text{PMe}_3$  was used to study the reaction profile. By using  $\text{PMe}_3$ , the reductive elimination transition state  $\text{TS}_{67\_Me}$  is 2.9 and 3.3 kcal/mol higher than the insertion transition state  $\text{TSB}\beta\_Me$  at B3LYP and BP86, respectively. In other words, the rate-determining step is reductive elimination using the bulkier phosphine ligand  $\text{PMe}_3$ . This is different from the palladium-catalyzed methylallene silaboration,<sup>34</sup> in which the rate-determining step is allene insertion into the Pd–B bond, using the internal carbon atom to attach to the boryl group. On the other hand, it is seen from Figure 5 that BP86 gives a much lower relative energy compared with B3LYP, in particular for transition states  $\text{TSB}\beta$  and  $\text{TS}_{67}$  (~10 kcal/mol lower). The situation that BP86 gives a lower transition barrier than B3LYP was also encountered in previous theoretical studies of oxidative addition of C–H,<sup>49</sup> C–C,<sup>50</sup> C–F,<sup>51</sup> and C–Cl<sup>52</sup> to Pd.

**F. Regioselectivities for Methylallene Bis-Selenation.** Since  $2B \rightarrow 4B \rightarrow \text{TSB}\beta \rightarrow 5B\beta$  is the most favorable pathway among the four allene insertion processes (Figure 2), the interactions of **2B** with methylallene have been studied to examine the regioselectivity of methylallene insertion. Scheme 2 shows the possible insertion reactions for methylallene. The complexes **4a–d** give the transition states **TSa–d**, which lead to the four corresponding insertion products **5a–d**, respectively. **a–d** represent four different positions of the methyl (Me) group on allene during methylallene insertions into the Pd–Se bond.

From Figure 7, it is seen that, among the four transition states of methylallene insertion, **TSc,d** are lower than **TSa,b**. **TSc** is only 0.2 kcal/mol lower than **TSd**. Among the four insertion products, **5c,d** are lower than **5a,b**. **5d** is only 0.8 kcal/mol lower than **5c**. Thus, the pathways  $2B \rightarrow 4c \rightarrow 5c$  and  $2B \rightarrow 4d \rightarrow 5d$  are competitive for methylallene insertion into the Pd–Se bond. Since the reductive elimination and allene insertion processes are comparable for allene bis-selenation as mentioned above, the processes from insertion products **5c,d** to reductive elimination transition states **TS67c,d** are investigated (Scheme 3). The reductive eliminations via **TS67c,d** would give the *Z* and *E* products **10c,d**, respectively.

From Figure 7, the reductive elimination transition states **TS67c,d** are higher than the corresponding insertion transition states **TSc,d**, respectively. **TS67c** is only 1.0 kcal/mol lower than **TS67d** from both B3LYP and BP86. Thus, the formations of the *Z* product **10c** and *E* product **10d** are competitive. This

is in agreement with the experimental results<sup>33</sup> that mixtures of *Z* and *E* isomers are obtained for allene bis-selenation.

**G. Influence of Carbon Monoxide.** The bis-selenation of allenes has been conducted in the presence of carbon monoxide in experiment.<sup>33</sup> Similarly, the isocyanide  $\text{ArNC}$  insertion into the Pd–Se bond<sup>56</sup> and CO insertion into the Pd–S bond<sup>57</sup> have been proposed experimentally for bis-selenation of isocyanide and azathiolation of carbon monoxide. Thus, it is interesting and necessary to examine the influence of carbon monoxide (CO). Since for the bis-selenation of allenes only the products with carbonyl attached to the internal carbon were obtained from experiment,<sup>33</sup> only the transition states related to the connection of carbon monoxide to the internal carbon atom of allene were examined.

When the Pd–C(O)SeMe bond was formed from CO insertion into the Pd–Se bond, the four possible transition states **TSA $\alpha$ \_CO**, **TSA $\beta$ \_CO**, **TSB $\alpha$ \_CO**, and **TSB $\beta$ \_CO** could be involved in allene insertion into the Pd–C(O)SeMe bond (Figure 8A,B). Among the four transition states for allene insertion into the Pd–C(O)SeMe bond, **TSB $\beta$ \_CO** is the most stable one, in which allene uses the internal carbon to connect to carbonyl of the trans complex  $\text{Pd}(\text{SeMe})[\text{C}(\text{O})\text{SeMe}](\text{PH}_3)$ . This is similar to allene insertion into the Pd–Se bond discussed above in which it is also the internal carbon attached to selenyl group of the trans complex  $\text{Pd}(\text{SeMe})_2(\text{PH}_3)$ .

When the Pd–C and C–Se bonds are formed from allene insertion into the Pd–Se bond, CO may activate the Pd–C or C–Se bond to generate the carbonylated products obtained from experiment.<sup>33</sup> The Pd–C bond is activated by CO at transition states **TSA1** and **TSB1** (Figure 8C), and the C–Se bond is activated at **TSA2** and **TSB2** (Figure 8D). In addition, there are other kinds of transition states, i.e., **TSA3** and **TSB3**, in which allene and CO simultaneously interact with the *cis* or *trans* complex  $\text{Pd}(\text{SeMe})_2(\text{PH}_3)$  (Figure 8E). The relative free energies of these transition states are presented in Figure 8. It is clear that **TSA1** and **TSB1** are the 2 lowest transition states among all the 10 transition states at B3LYP and BP86 levels, whereas **TSA2** and **TSB2** are the 2 highest transition states. This indicates that the Pd–C bond is more easily activated by CO than is the C–Se bond, in agreement with suggestions of CO insertion into Pd–C bonds<sup>13,17,24,58,59</sup> or Pt–C bonds.<sup>18</sup>

As an alternative important process for CO introduction, the phosphine ligand on  $\text{Pd}(\text{SeMe})_2(\text{PH}_3)$  may be replaced with CO by a ligand-exchange reaction to form  $\text{Pd}(\text{SeMe})_2(\text{CO})$ . The corresponding transition states were examined. For CO replacing  $\text{PH}_3$  in *cis*- $\text{Pd}(\text{SeMe})_2(\text{PH}_3)$ , the corresponding transition state was calculated to be 3.0 kcal/mol higher at the B3LYP level (5.6 kcal/mol at the BP86 level) than the most stable transition state **TSA1**. However, for CO replacing  $\text{PH}_3$  in *trans*- $\text{Pd}(\text{SeMe})_2(\text{PH}_3)$ , our efforts to locate the corresponding transition state failed. Therefore, further calculations were not performed.

**TSA1** is the transition state after the coordination of CO to the open site of the Pd atom of complex **5A $\alpha$**  (Figure 2A). In other words, CO might coordinate to the open site of the Pd atom of complex **5A $\alpha$**  and then attack the Pd–C bond generated from allene insertion into the Pd–Se bond of *cis*-

(56) Kuniyasu, H.; Maruyama, A.; Kurosawa, H. *Organometallics* **1998**, *17*, 908.

(57) Kuniyasu, H.; Hiraike, H.; Morita, M.; Tanaka, A.; Sugoh, K.; Kurosawa, H. *J. Org. Chem.* **1999**, *64*, 7305.

(58) Knapton, D. J.; Meyer, T. Y. *J. Org. Chem.* **2005**, *70*, 785.

(59) Kuniyasu, H.; Kato, T.; Asano, S.; Ye, J.-H.; Ohmori, T.; Morita, M.; Hiraike, H.; Fujiwara, S.; Terao, J.; Kurosawa, H.; Kambe, N. *Tetrahedron Lett.* **2006**, *47*, 1141.

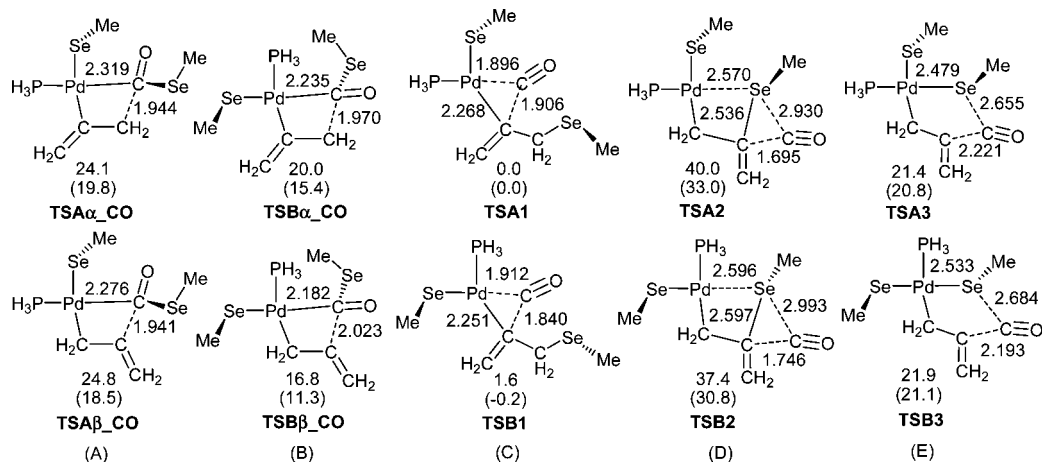
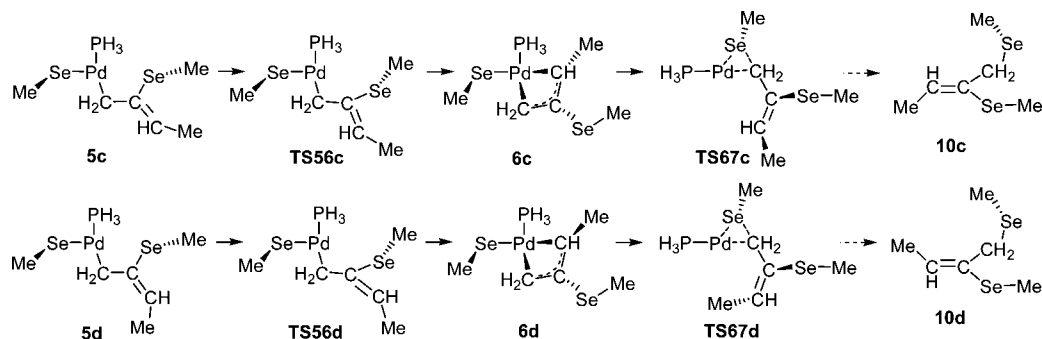


**Figure 8.** Geometries (Å) of the transition states for allene insertion into the Pd–C(O) bond (**TSA $\alpha$ \_CO**, **TSA $\beta$ \_CO**, **TSB $\alpha$ \_CO**, **TSB $\beta$ \_CO**) and CO insertion into the Pd–C (**TSA1**, **TSB1**) or C–Se (**TSA2**, **TSB2**) bond, as well as CO and allene interaction with Pd(SeMe)<sub>2</sub>(PH<sub>3</sub>) simultaneously (**TSA3**, **TSB3**). The energy values (in kcal/mol) are the relative free energies from B3LYP, while those in parentheses are from BP86. All values are relative to **TSA1**.

### Scheme 3. Proposed Mechanism for Isomerization Steps with Methylallene



Pd(SeMe)<sub>2</sub>(PH<sub>3</sub>) (**2A**) via transition state **TSA1**. Similarly, **TSB1** is the transition state after the coordination of CO to the open site of the Pd atom of complex **5B $\alpha$**  (Figure 2B). From Figure 2, it is interesting to note that, although **TSB $\beta$**  is lowest in energy among the four transition states (**TSA $\alpha$** , **TSA $\beta$** , **TSB $\alpha$** , and **TSB $\beta$** ) of allene insertion into the Pd–Se bond, the carbonylation process proceeds to follow the pathway of **5A $\alpha$**  or **5B $\alpha$**  due to the preference of Pd–C bond activation over C–Se bond activation by CO (Figure 8C,D). Thus, the most favorable pathway for CO introduction might be as follows: CO coordinates the  $\sigma$ -vinyl palladium complex **5A $\alpha$**  (or **5B $\alpha$** ) and then the Pd–C bond is activated by CO, giving a complex with carbonyl at the internal carbon, which successively forms the final carbonylating product as in experiment<sup>33</sup> by a reductive elimination process.

In previous studies, the catalytic addition of a S–H bond<sup>14,17–21</sup> or E–E ( $E = S, Se$ ) bond<sup>12,13,58</sup> to alkynes had been performed under pressurized carbon monoxide to investigate the addition mechanism or to obtain the carbonylated products. Thus, we hope our findings of the influence of CO on the reaction mechanism might provide useful information for further understanding these reactions in the presence of carbon monoxide and developing new addition reactions of group 16 heteroatom compounds to unsaturated organic molecules.

## IV. Conclusions

The Pd(0)-catalyzed allene bis-selenation reaction has been studied by using the hybrid B3LYP and pure BP86 DFT methods. Both methods give consistent results. The most favored reaction pathway proceeds via the following steps: (a) oxidative

addition of Se–Se to Pd(PH<sub>3</sub>)<sub>2</sub> to generate the cis complex Pd(SeMe)<sub>2</sub>(PH<sub>3</sub>)<sub>2</sub>, (b) dissociation of PH<sub>3</sub> from *cis*-Pd(SeMe)<sub>2</sub>(PH<sub>3</sub>)<sub>2</sub> to form *cis*-Pd(SeMe)<sub>2</sub>(PH<sub>3</sub>), (c) isomerization of the cis complex to the complex *trans*-Pd(SeMe)<sub>2</sub>(PH<sub>3</sub>), (d) allene coordination and insertion into the Pd–Se bond of *trans*-Pd(SeMe)<sub>2</sub>(PH<sub>3</sub>) using the internal carbon atom attached to the selenyl group, (e) isomerization from the  $\sigma$ -allyl to  $\pi$ -allyl complex, and (f) reductive elimination to give the final product (Z)-CH<sub>2</sub>=C(SeMe)CH<sub>2</sub>(SeMe). With the PH<sub>3</sub> ligand, allene insertion and reductive elimination are competitive for the rate-determining step, while the rate-determining step is the reductive elimination process with the bulkier PMe<sub>3</sub>. This suggests the importance of the ligand effect.

For methylallene, the *Z* and *E* isomers of the Se–Se bond addition products are formed in a competitive way, in agreement with experiment. The formation of carbonylating products involves CO insertion into the Pd–C bond of the cis or *trans*  $\sigma$ -vinyl palladium complex generated from allene insertion into the Pd–Se bond.

**Acknowledgment.** We thank the National Natural Science Foundation of China for financial support (Grant 20773117).

**Supporting Information Available:** Tables giving Cartesian coordinates of allene and methylallene bis-selenation catalyzed by Pd(PH<sub>3</sub>)<sub>2</sub> and CO introduction from the B3LYP-optimized geometries. This material is available free of charge via the Internet at <http://pubs.acs.org>.

OM801074S